August 27-31, 2023
FLORENCE - ITALY
16th International Conference on Wind Engineering
ICWE 16

# Modal effects on flutter of long-span suspension bridges

Yan Zhang [1], Haili Liao [1]

[1]Research Center for Wind Engineering of Southwest Jiaotong University, Chengdu, China,
Y_Zhang@my.swjtu.edu.cn

**SUMMARY:**
The critical wind speed of segment model flutter (2-DOF flutter) is often different from that of full aeroelastic model flutter (3D flutter), and the aim of this paper is to find out the reason for the difference. Five suspension bridges with different main girder support forms were taken as examples herein, the characteristics of 3D flutter for these suspension bridges were analysed by 3D multi-mode flutter analysis method, and the differences between 2-DOF flutter and 3D flutter were studied according to the similarities between vertical-bending modes and torsional modes as well as energy ratios of flutter participating vibration modes. The flutter mechanisms for long-span suspension bridges are summarized as follows: the energy ratio of a vertical-bending vibration mode is positively related to the similarity between this vertical-bending vibration mode and 1st torsional vibration mode; the 2-DOF flutter critical wind speed will be higher than the 3D flutter critical wind speed for single-span simply supported suspension bridge but the situation will be the opposite for multi-spans continuously supported suspension bridge if segment model wind tunnel test simulates the basic vertical-bending vibration mode and basic torsional vibration mode of the bridge.

*Keywords: long-span suspension bridges, flutter characteristics, modal effects*

## 1. GENERAL INSTRUCTIONS

The flutter performance of a long-span suspension bridge needs to be tested to avoid the occurrence of aerodynamic instability, the test methods include wind tunnel tests of segment models and full aeroelastic models. Segment model tests are usually conducted for main girders' aerodynamic shape optimizations and preliminary predictions of flutter critical wind speeds; full aeroelastic model tests are usually conducted for the final checks of aerodynamic instability. Segment model systems simplify 3D real bridges into 2-DOF vibration systems, which cause the differences in critical wind speeds between 2-DOF flutter and 3D flutter. Researchers (Ma et al., 2021) have found that 2-DOF flutter critical wind speeds are significantly higher than 3D flutter critical wind speeds for some suspension bridges. It is always expected that the 2-DOF flutter critical wind speeds be lower than 3D flutter critical wind speeds, which implies the preliminary estimations of aerodynamic instability based on segment model tests could be conservative for long-span suspension bridges. According to available study (Ma et al., 2021), what cause the difference between 2-DOF flutter and 3D flutter are 3D aeroelastic effects including multi-mode coupled effect, lateral self-excited aerodynamic force effect, aerodynamic effect of main cables, additional static wind angle of attack effect and stiffness degradation effect of main cables. Multi-mode coupled effect is the key factor for the difference, as a result the paper is aiming at researching the modal effects on flutter of long-span suspension bridges.

## 2. 3D FLUTTER ANALYSIS BASED ON AERODYNAMIC FORCE OF IDEAL THIN PLATE

### 2.1. Objects of Study

Five long-span suspension bridges with different main girder support forms are taken as the objects of study, their structural features are shown in Fig. 1 and Table 1. The 3D multi-mode coupled flutter analysis program **MCFAN**, based on state-space method (Ding et al., 2002), is programmed for 2-DOF flutter analysis and 3D flutter analysis in paper. Flutter derivatives of ideal thin plate are used for flutter analysis to avoid acquisition errors of aerodynamic derivatives.

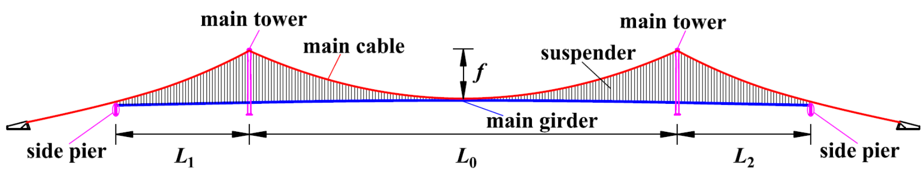


**Figure 1.** Structural diagram of long-span suspension bridge.

**Table 1.** Structural features of suspension bridges.

| Support form of main girder | Example number | Length of $L_0$/m | $L_0/f$ | Length of $L_1$ and $L_2$/m | |
|---|---|---|---|---|---|
| | | | | $L_1$ | $L_2$ |
| Single-span simply supported | I | 916 | 11.06 | 0 | 0 |
| | II | 1208 | 9.28 | 0 | 0 |
| | III | 2100 | 9.76 | 0 | 0 |
| Three-spans continuously supported | IV | 1666 | 9.65 | 500 | 500 |
| Two-spans continuously supported | V | 2300 | 9.00 | 0 | 717 |

### 2.2. 3D Flutter Analysis of Suspension Bridges

The modal properties of five suspension bridges are calculated by **ANSYS** firstly, and then the first 30-orders modal property parameters and flutter derivatives of ideal thin plate are input into **MCFAN** for flutter analysis. The flutter critical wind speed ($U_{cr}$ for short), the flutter frequency ($f_{cr}$ for short) and the energy ratios of flutter participating vibration modes ($e$ for short) are shown in Fig. 2 and Table 2. It can be seen from Fig. 2 that there are obvious contrasts between single-span suspension bridges and multi-spans suspension bridges as for energy ratios of vertical-bending vibration modes: the energy ratio of basic vertical-bending vibration mode, V-S-1, is dominant while the energy ratios of higher-order vertical-bending vibration modes, V-S-2 and V-S-3, are quite small for multi-spans suspension bridges; the energy ratio of 2nd vertical-bending vibration mode, V-S-2, is equivalent to or greater than that of basic vertical-bending vibration mode, V-S-1, for single-span suspension bridges.

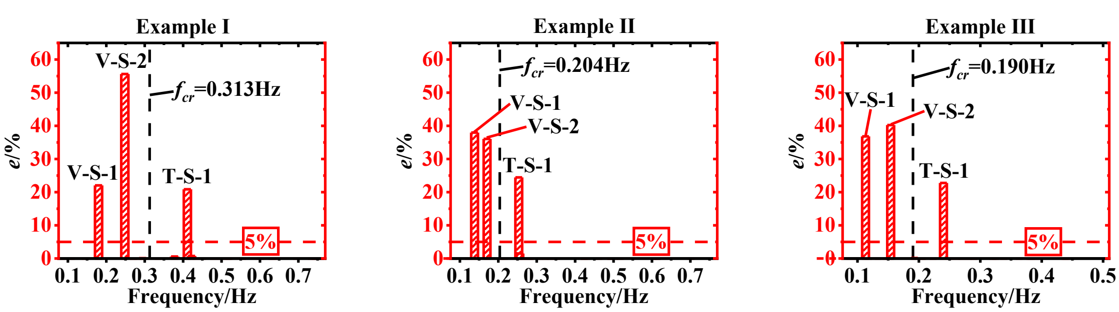

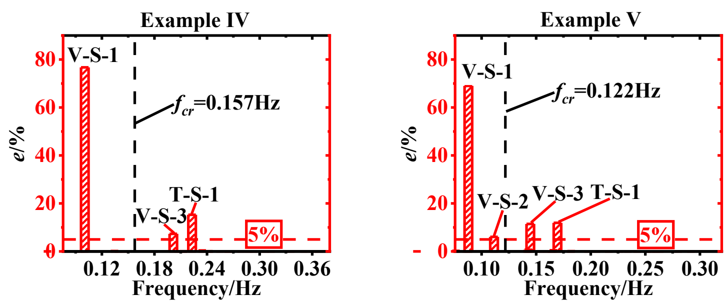


**Figure 2.** Flutter frequencies and energy ratio of flutter participating vibration modes.

Flutter critical wind speeds and flutter frequencies with different combinations of vibration modes are shown in Table 2. The flutter critical wind speeds decrease and the flutter frequencies increase with the participation of 2nd vertical-bending vibration modes for single-span suspension bridges drastically. The flutter critical wind speeds increase slightly and the flutter frequencies change a little with the participation of higher-order vertical-bending vibration modes for multi-spans suspension bridges.

**Table 2.** Flutter critical wind speeds and flutter frequencies with different combinations of vibration modes.

| Combination of vibration modes | $U_{cr}$/(m·s$^{-1}$) | | | | | $f_{cr}$/Hz | | | | |
|---|---|---|---|---|---|---|---|---|---|---|
| | I | II | III | IV | V | I | II | III | IV | V |
| V-S-1+T-S-1 | 108.3 | 92.6 | 153.5 | 85.2 | 62.0 | 0.243 | 0.188 | 0.173 | 0.161 | 0.124 |
| V-S-1,2+T-S-1 | 87.7 | 82.3 | 136.5 | 85.1 | 61.5 | 0.315 | 0.205 | 0.190 | 0.161 | 0.125 |
| V-S-1,2,3+T-S-1 | 88.0 | 82.3 | 136.6 | 87.9 | 64.8 | 0.315 | 0.205 | 0.190 | 0.158 | 0.122 |
| Full modes (first 30 orders) | 87.2 | 81.2 | 136.6 | 87.9 | 64.2 | 0.313 | 0.204 | 0.190 | 0.157 | 0.122 |

## 2.3. Similarity between Vertical-bending Vibration Mode and Torsional Vibration Mode

The better similarity between a vertical-bending vibration mode and a torsional vibration mode means the higher coupling degree between these two vibration modes during flutter (Xie and Xiang, 1987). $D_{f,\Phi}$, as shown in Eq. (1), represents the similarity between a vertical-bending mode shape $f(x)$ and a torsional mode shape $\Phi(x)$. The two mode shapes are completely similar if $D_{f,\Phi}$=1. $D_{f,\Phi}$ between symmetrical vertical-bending vibration modes and 1st symmetrical torsional vibration mode are shown in Table 3. The energy ratio of a vertical-bending vibration mode is positively related to the similarity between this vertical-bending vibration mode and 1st torsional vibration mode.

$$D_{f,\Phi}=\sqrt{\left[\int_0^{L_0+L_1+L_2} f(x)\cdot\Phi(x)\mathrm{d}x\right]^2\Big/\left[\int_0^{L_0+L_1+L_2} f^2(x)\mathrm{d}x\cdot\int_0^{L_0+L_1+L_2}\Phi^2(x)\mathrm{d}x\right]} \tag{1}$$

**Table 3.** $D_{f,\Phi}$ between symmetrical vertical-bending vibration modes and 1st symmetrical torsional vibration mode.

| $f$ | $\Phi$ | $D_{f,\Phi}$ | | | | |
|---|---|---|---|---|---|---|
| | | I | II | III | IV | V |
| V-S-1 | | 0.71 | 0.85 | 0.86 | 0.94 | 0.92 |
| V-S-2 | T-S-1 | 0.70 | 0.53 | 0.50 | 0.02 | 0.15 |
| V-S-3 | | 0.08 | 0.01 | 0.04 | 0.33 | 0.35 |

## 3. DIFFERENCE BETWEEN 2-DOF FLUTTER AND 3D FLUTTER

Flutter critical wind speeds for five suspension bridges, which calculated by using the flutter derivatives of ideal thin plate, are shown in Fig. 3(a). The 3D flutter critical wind speeds are slightly lower than 2-DOF flutter critical wind speeds with V-S-1+T-S-1 as combination of vibration modes but slightly higher than 2-DOF flutter critical wind speeds with V-S-2+T-S-1 as combination of vibration modes for single-span suspension bridges. The 3D flutter critical wind speeds are slightly higher than 2-DOF flutter critical wind speeds with V-S-1+T-S-1 as combination of vibration modes for multi-spans suspension bridges. The flutter critical wind speeds for suspension bridges whose main girder is a streamlined box girder at large initial angle of attack, taking +5° initial angle of attack as an example, are shown in Fig. 3(b). It is thus clear that the relationships for flutter critical wind speeds shown in Fig. 3(b) are similar with Fig. 3(a).

Flutter critical wind speeds for suspension bridges whose main girder is a double box composite beam are shown in Fig. 3(c). The cross section of double box composite beam is shown in the literature (Ge and Tanaka, 2000). The critical wind speeds for 3D flutter and 2-DOF flutter are quite the same in Fig. 3(c), which is different from the relationships shown in Fig. 3(a) and Fig. 3(b). This is owing to thin plate or streamlined box girder suspension bridge, featured as bending-torsional coupled flutter, is evidently influenced by vertical-bending vibration modes but double box composite beam suspension bridge, featured as torsional flutter, is basically not influenced by vertical-bending vibration modes.

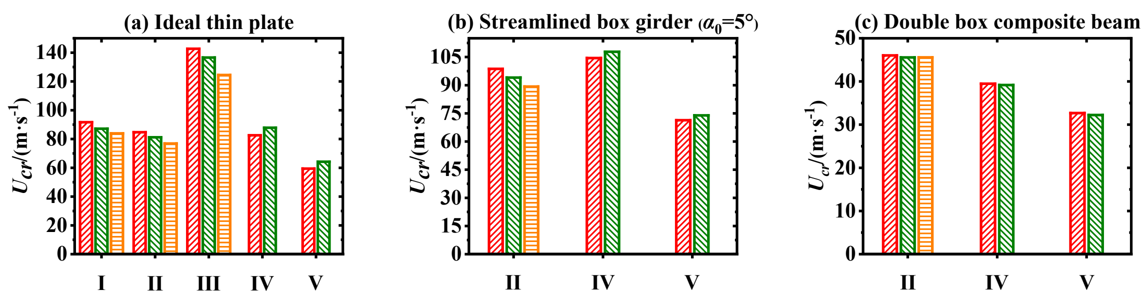


**Figure 3.** *Ucr* (▨: 2-DOF flutter (V-S-1+T-S-1); ▤: 2-DOF flutter (V-S-2+T-S-1); ▧: 3D flutter).

## 4. CONCLUSIONS

The basic symmetric torsional vibration mode and the first several symmetric vertical-bending vibration modes are major flutter participating modes for long-span suspension bridges, and the energy ratio of a vertical-bending vibration mode is positively related to the similarity between this vertical-bending vibration mode and 1st torsional vibration mode. When conducting segment model wind tunnel test, the modes combination of V-S-2 and T-S-1 can obtain a conservative flutter critical wind speed for single-span suspension bridges and so do the modes combination of V-S-1 and T-S-1 for multi-spans suspension bridges.

**REFERENCES**

Ding, Q., Chen, A., and Xiang, H., 2002. Coupled flutter analysis of long-span bridges by multimode and full-order approaches. Journal of Wind Engineering and Industrial Aerodynamics 90, 1981–1993.

Ge, Y. and Tanaka, H., 2000. Aerodynamic flutter analysis of cable-supported bridges by multi-mode and full-mode approaches. Journal of Wind Engineering and Industrial Aerodynamics 86, 123–153.

Ma, T., Zhao, L., and Shen, X., 2021. Case study of three-dimensional aeroelastic effect on critical flutter wind speed of long-span bridges. Journal of Wind Engineering and Industrial Aerodynamics 212, 104614.

Xie, J. and Xiang, H., 1987. New concepts on wind-resistant design of bridges—multi-mode coupled flutter. China Civil Engineering Journal 20(2), 35–45.